Elsevier Editorial System(tm) for The Veterinary Journal
Manuscript Draft

Manuscript Number: YTVJL-D-10-00623R2

Title: Application of high-frequency ultrasound for the detection of surgical anatomy in the rodent abdomen

Article Type: Original Article

Keywords: Rat abdomen, High-frequency ultrasound, Anatomy, Living image

Corresponding Author: Professor Chuan-Mu Chen, Ph.D.

Corresponding Author's Institution: National Chung Hsing University

First Author: Jiun-Yu Chen, Ph.D.

Order of Authors: Jiun-Yu Chen, Ph.D. ; Hsiao-Ling Chen, Ph.D.; Sheng-Hai Wu, Ph.D.; Tung-Chou Tsai, Ph.D.; Ming-Fong Lin, M.D.; Chih-Ching Yen, M.D., Ph.D.; Wu-Huei Hsu, M.D.; Wei Chen, M.D.; Chuan-Mu Chen, Ph.D.

Abstract: Rats are used extensively in abdominal disease research. To monitor disease progress in vivo, high-frequency ultrasound (HFU) can be a powerful tool for obtaining high-resolution images of biological tissues. However, there is a paucity of data regarding the correlation between rat anatomy and corresponding HFU images. Twenty-four adult male Sprague-Dawley (SD) rats underwent abdominal scans using high-frequency ultrasound (40-MHz) surgical procedures to identify abdominal organs and major vessels as well as in situ scanning to confirm the imaging results. The results were compared with those of human abdominal organs in ultrasonographic scans. The rat liver, paired kidneys, stomach, intestines, and major blood vessels were identified by HFU. The ultrasonic morphologies of the liver and kidneys showed differences between rats and humans. Clinically relevant anatomical structures were identified using HFU imaging of the rat abdomen, and these structures were compared with the corresponding structures in humans. Increased knowledge with regard to identifying the anatomy of rat abdominal organs by ultrasound allows scientists to conduct more detailed intra-abdominal research in rodents.

**Original article**

# Application of high-frequency ultrasound for the detection of surgical anatomy in the rodent abdomen

J.Y. Chen [a,†], H.L. Chen [b,†], S.H. Wu [a], T.C. Tsai [a], M.F. Lin [a,c], C.C. Yen [a,d], W.H. Hsu [d], W. Chen [a,e,*], C.M. Chen [a,f,*]

[a] *Department of Life Sciences, National Chung Hsing University, Taichung 402;*

[b] *Department of Molecular Biotechnology, Da-Yeh University, Changhwa 515;*

[c] *Taichung Hospital, Department of Health, Taichung 403;*

[d] *Department of Internal Medicine, China Medical University Hospital, Taichung 404;*

[e] *Department of Internal Medicine, Chia-Yi Christian Hospital, Chia-Yi 600;*

[f] *School of Chinese Medicine, China Medical University, Taichung, 404; Taiwan*

[†]These authors contributed equally to this work

* Corresponding authors: Tel.: +886 4 2285 6309; fax: +886 4 2285 1797.

*E-mail address*: chchen1@dragon.nchu.edu.tw (C.M. Chen) or peteralfa2004@yahoo.com.tw (W. Chen)

**Abstract**

Rats are used extensively in abdominal disease research. To monitor disease progress in vivo, high-frequency ultrasound (HFU) can be a powerful tool for obtaining high-resolution images of biological tissues. However, there is a paucity of data regarding the correlation between rat anatomy and corresponding HFU images. Twenty-four adult male Sprague-Dawley (SD) rats underwent abdominal scans using high-frequency ultrasound (40-MHz) surgical procedures to identify abdominal organs and major vessels as well as in situ scanning to confirm the imaging results. The results were compared with those of human abdominal organs in ultrasonographic scans. The rat liver, paired kidneys, stomach, intestines, and major blood vessels were identified by HFU. The ultrasonic morphologies of the liver and kidneys showed differences between rats and humans. Clinically relevant anatomical structures were identified using HFU imaging of the rat abdomen, and these structures were compared with the corresponding structures in humans. Increased knowledge with regard to identifying the anatomy of rat abdominal organs by ultrasound allows scientists to conduct more detailed intra-abdominal research in rodents.

*Keywords:* Rat abdomen; High-frequency ultrasound; Anatomy; Living image

## Introduction

Experimental models using small animals are receiving increasing recognition as a powerful means of study in genomics research, disease research, pharmacological research and molecular biology (Feldman and Brunner, 1994; Poltorak et al., 1998; Van Rhijn et al., 2008). The ability to reproduce human disease using such models has been proven, providing researchers with new diagnostic and therapeutic approaches. Thus, the development of a non-invasive modality for small-animal imaging is critically important because it may provide the possibility of longitudinal research on the same animal, shortened observation times, and reduced requirements for animal sacrifice (Grassi et al., 2009). Several non-invasive devices have been developed recently for small-animal experiments, including ultrasound, magnetic resonance (MR), computed tomography (CT), single photon emission computed tomography (SPECT) and positron emission tomography (PET). Among these devices, ultrasound has the advantages of low cost, rapid imaging speed, portability and high resolution (Foster et al., 2002).

Ultrasound techniques have aided the diagnosis of human diseases for decades, especially with regard to hepatology (Robinson, 2008; Wieckowska and Feldstein, 2008), gastroenterology (Nylund et al., 2009), pulmonology ( Yang, 2000; Tsai and

Yang, 2003), cardiology (Kpodonu et al., 2008), gynaecology (Benacerraf et al., 2005), and nephrology (Mostbeck et al., 2001). However, the applications of ultrasound in small-animal research have been limited by its resolution because conventional ultrasonic imaging systems for humans typically use a frequency range of 2 - 15 MHz. To improve spatial resolution, one strategy would be to increase the ultrasound frequency. Due to technical advances, high-frequency ultrasound (HFU), which refers to frequencies above 20 MHz, has become more readily available (Foster et al., 2000; Knspik et al., 2000; Goertz et al., 2003). HFU provides non-invasive, real-time images with a spatial resolution of less than 100 μm.

Significant research efforts have been directed toward liver and kidney diseases and have used rats as animal models. Such diseases include hepatocellular carcinoma (Lu et al., 2009), liver cirrhosis (de Lima et al., 2008), obstructive uropathy (Chuang et al., 2000), and nephritis (Jaimes et al., 2009). In these models, ultrasound could be a useful tool for evaluating disease progression and pharmacological effects (Fleck et al., 2002; Lee et al., 2005). However, there is a paucity of data regarding the correlation between rat abdominal anatomy and the corresponding images obtained using high-frequency ultrasound.

The aim of this study was to describe and identify rat abdominal organs (including the liver, kidneys, stomach, and spleen) using HFU. To obtain these images, a commercially available ultrasonic imaging system (Visual Sonics Vevo 770) was used. The results of rat imaging were then correlated with human anatomical structures.

## Materials and methods

### *Animals*

Twenty-four male Sprague-Dawley (SD) rats weighing 250-300 g were used. Animals were housed at a controlled temperature (23 $^{o}$C) with a daily exposure to a 12-h: 12-h light-dark cycle (Yen et al., 2009). The animal use protocol in this study has been reviewed and approved by the Institutional Animal Care and Use Committee of the National Chung Hsing University (IACUC Approval number: 97-54).

### *Study protocol*

To thoroughly understand rat abdominal organ anatomy, we reviewed relevant published studies (Corman et al., 1985; Morehouse et al., 1995; Kogure et al., 1999; Madrahimov et al., 2006; Martins and Neuhaus, 2007). After completing our review of rat abdominal anatomy, we performed ultrasound scanning and recorded images.

Thereafter, the rats were sacrificed, and the transducer was placed in direct contact with the organs to confirm the results of the images obtained using ultrasound.

*HFU examination*

During the surgical procedures, animals were lightly anesthetised with gas consisting of 0.5-1 L/min of oxygen-enriched air mixed with 2.0-2.5% isoflurane vapour. The animals were fasted for 3 h prior to high-frequency ultrasound (HFU) scanning. The animals were placed in supine positions and were breathing spontaneously. After being anesthetised, each rat abdomen was shaved and further cleaned with a chemical hair remover to minimize ultrasound attenuation. Typical diagnostic scanners emit ultrasound at frequencies ranging from 2-15 MHz. This range of frequencies cannot provide sufficient resolution to the image axons. Therefore, a commercially available HFU apparatus (Visual Sonics Vevo 770 with the RMV 704) was used in this experiment. A transducer that was used for imaging rat abdominal organs had a central frequency of 40 MHz and provided an axial resolution of 40 μm with a 14.6-mm field of view. Ultrasound gel was placed on the skin as a coupling fluid before using the transducer.

Areas of key importance to this study were those where the data provided by in

situ images corresponded with those obtained from the rat abdominal tissues. Thus, for both control and experimental animals, abdominal tissues were imaged in situ through the overlying musculature. This overlying musculature was then held apart with surgical spreaders, and the animals were sacrificed. The exposed abdominal tissues were then imaged by applying the ultrasound probe.

*Surgical procedure and identification of rat anatomy*

After the ultrasound examination, each rat underwent a surgical procedure for anatomy identification. In anesthetized rats, midlaparotomies were followed by lateral transverse incisions. Then, the liver ligaments were incised. The intestinal loops were dissected to show the liver, kidneys and inferior vena cava (Fig. 1). Euthanasia was performed after anatomic dissection.

## Results

*Anatomy and ultrasonographic presentations of rat kidneys*

Anatomy: in rats, paired kidneys were located behind the intestinal loops, one on each side of the spine. As shown in Fig. 1, the right kidney was situated just below the inferior right lobe (IRL) of the liver, and the left kidney was situated below the left lateral lobe (LLL) of the liver and posterior to the stomach. The asymmetry caused by

the liver within the abdominal cavity typically resulted in the left kidney being slightly lower than the right. This arrangement was opposite that of human kidneys. Each kidney weighed between 1.8 and 2.2 g and had a transverse diameter measuring between 8 and 10 mm.

Ultrasound examination: in rats, the right kidney was a good landmark for the initiation of ultrasonic scanning. The examination began just below the right lowest rib in the transverse plane (Fig. 2a), and the transducer was moved slightly and slowly around that region to locate the right kidney. On ultrasound, the kidney appeared as an oval with a longitudinal diameter measuring between 11 and 14 mm and a transverse diameter measuring between 7.5 and 8.0 mm. By tilting and moving the transducer leftward slightly, it was possible to locate the portion of the liver that surrounded the right kidney. This portion of the liver was the inferior right lobe (Fig. 2b and 2d). The central potion (medulla) was relatively hyperechogenic due to the abundant interfaces produced by the blood vessels and drainage system. In this portion, there were a few relatively hypoechoic pyramids that were surrounded by the cortical layer (Fig. 2c and 2e). The kidney was scanned in at least two planes to adequately visualize all of the parenchyma and supplying blood vessels. Two main vessels passed through this region from the medulla to the hilum; one was the renal artery, and the other was the

renal vein. We were able to identify the renal artery using Doppler ultrasound, which demonstrated a frequency shift during systole with a gradual decrease in flow throughout diastole. On the other hand, the renal vein flow was constant throughout the cardiac cycle.

*Anatomy and ultrasonographic presentations of the rat liver*

Anatomy: in rats, the liver was the largest internal organ, accounting for approximately 5% of the total bodyweight (BW). It was a soft, pinkish-brown, multilobed organ, located in the right and left upper quadrants of the abdominal cavity, resting just below the diaphragm (Fig. 1). In rat liver weighting range from 9.6 to 13.5 g, the liver's mean weight was 12.5 g. Gross anatomy divided the liver into four major lobes, the median lobe, the right lobe, the left lobe and the caudate lobe. These divisions were based on surface features. In Fig. 1, the caudate lobe (CL) was not visible because it was situated behind the left lateral lobe (LLL). The median lobe (ML) was located just below the diaphragm and was sub-divided by a main fissure into a right medial lobe (RML) and a left medial lobe (LML). The right lobe was located to the right of the vena cava and was almost completely covered by the medial lobe. The rat liver was further divided by a horizontal fissure into two lobules: the superior right lobe (SRL) and the inferior right lobe (IRL).

Ultrasound examination: after scanning for the right kidney, the transducer was moved leftward slightly in a transverse plane near the midline. It was possible to see the relative position between the inferior vena cava (IVC) and the hepatic vasculature (Fig. 3). The extrahepatic portal vein was located posterior and lateral to the hepatic artery (HA) and the common bile duct (CBD). Then, by moving the transducer upward near the xiphoid, the right part of the liver was visible (Fig. 4a). The margin of the right liver was smooth and wedge-shaped, and the corresponding region was the RML (Fig. 4b and 4e). The liver parenchyma had a uniform, sponge-like texture of low-level echogenicity. Passing through it were the blood vessels, which were seen as branching tubular structures that could be traced toward the porta (portal veins; PV) or the hepatic veins (IVC). Portal veins were usually surrounded by reflective tissue, whereas hepatic veins usually appeared as simple hypoechoic tubular structures (Fig. 4c and 4f). By moving the transducer slightly toward the midline, one could observe that the SRL lay posterior to the RML near a fissure (Fig. 4d and 4g).

By moving the transducer just across the midline (Fig. 5a), one could see that the LML is near the left side of the RML. A vertical fissure, called the main fissure or umbilical fissure, was located between the two lobes (Fig. 5b and 5d). At this location,

a compression manoeuvre was used to image the deeper part of the liver. Then, it was possible to observe the pulsating aorta and portal triad in this section (Fig. 5c and 5e). By moving the transducer to the left (Fig. 6a), a wedge-shaped border of the left liver (LLL) could be seen (Fig. 6b and 6d). After tilting the transducer slightly and in a hyperechoic curve line below the LLL, the stomach was visible (Fig. 6c and 6e).

*Anatomy and ultrasonographic presentations of the rat spleen*

Anatomy: the spleen lay in the left upper quadrant of the abdomen, immediately beneath the left hemi-diaphragm (Fig. 1). It was an approximately triangular organ and was fixed by ligaments in a position between the left diaphragm and the stomach.

Ultrasound examination: after scanning for the left portion of the liver, the transducer was moved laterally and caudally to locate the spleen, which was observed as a triangular organ with evenly distributed fine echoes (Fig. 7a). The best landmark in this case was the left kidney, which lay caudal to the spleen and was readily identified by its distinct sonographic pattern (Fig. 7b and 7c).

## Discussion

Micro-ultrasound has proven to be a useful tool for monitoring and assessing

abdominal diseases in small animals (Chuang et al., 2000; de Lima et al., 2008; Jaimes et al., 2009; Lu et al., 2009; Sullivan et al., 2009). Thus, detailed scanning techniques and a thorough description and identification of anatomy by ultrasound are crucial when designing and performing experiments with regard to the rat abdomen. To our knowledge, this is the first study investigating the correlation between ultrasonic imaging and rat abdominal anatomy using high-frequency ultrasound (40-MHz). In this study, we report our experiences with scanning technique to clearly identify abdominal organs by HFU.

Scanning abdominal organs in rats is much more difficult than scanning humans because of the faster respiratory rates of rats (approximately 90 breaths / min). Thus, the images on the screen swing constantly despite the rat being under anaesthesia. A novice performing the ultrasound procedure must overcome this difficulty. Even using a mini-transducer, scanning should be conducted very slowly and steadily; otherwise, tiny organs could be missed.

The best landmark in rat abdominal ultrasound examinations was probably the right kidney, which lay inferior to the right diaphragm and could be identified easily by its distinct ultrasonographic patterns (Fig. 2a and 2b). Relative to their

identification in humans, it was much easier to identify both kidneys by ultrasound in rats when they are placed in the supine position. Because human kidneys are located in the retroperitoneal cavity, obtaining optimal views sometimes requires subjects to lie in a decubitus or prone position. The kidney also differs significantly in their ultrasonographic demonstrations between rats and humans. The rat kidney did not show an obvious border between the medulla and the cortex, whereas the human kidney was strongly echogenic in the central portion and had hypoechoic surroundings (Fig. 8a, right panel). In addition, it was easy to scan the main blood vessels passing through the rat kidney (Fig. 2c), but it was rare to see these features during human ultrasounds. Thus, future studies may include measurements of the intra-renal artery resistance index by Doppler to evaluate the severity of kidney injuries.

Ultrasound has proven to be an effective tool for monitoring and assessing hepatomas (Yang et al., 1993; Oh et al., 2002; Di Stefano et al., 2008) and liver cirrhosis (Yan et al., 2007; de Lima et al., 2008; Dias et al., 2008) in small animal experiments. However, it is difficult to scan the rat liver properly because it is easy to flatten the liver by compression (Fig. 5b and 5c). Thus, we suggest first scanning the liver lightly and gently and then applying pressure to the organ to examine deeper

areas.

The greatest difference between the hepatobiliary systems of rats and humans is the fact that the rat has no gallbladder (Fig. 8a, left panel). In humans, Murphy's point in the right upper quadrant refers to the gallbladder, and this is a useful landmark for guidance to specific target organs (Taylor et al., 1976). In addition, human liver lobes have no clear fissure lines or divisions under ultrasonographic depictions, whereas rat livers show multiple lobes with clear fissures between them (Fig. 4d and 5b). The differences in ultrasound imaging between rats and humans are summarised in Table 1.

The ultrasonographic pattern of the rat spleen (Fig. 7b) was very similar to that of the human spleen (Fig. 8b). Both are triangular in shape and exhibit evenly distributed, fine echoes. The pancreas is not difficult to find during a human ultrasound, but we could not identify the rat pancreas in our study.

HFU technique has inherent limitations. The images have a limited depth of field because of the short wavelength and the low fixed F-number of conventional transducers (Mamou et al., 2009). However, in our investigation, we could still scan

most abdominal organs thoroughly using various scanning techniques, such as tilting, compression, and rotation of the transducer.

## Conclusions

In conclusion, the rat is the most commonly used experimental model for simulating abdominal diseases. The employment of high-frequency ultrasound requires detailed knowledge of regional abdominal anatomy and optimal scanning techniques. In this study, we identified the anatomy of the kidneys, liver, stomach, and spleen in situ immediately. By the knowledge, we may observe the process of tissue regeneration or severity of tissue injury of the abdominal organs more accurately in the future. The data show that sonography, with a resolution of 40 μm, permits observation of hepatic repair and kidney regeneration processes in rats.

## Conflict of interest statement

None of the authors has any financial or personal relationships that could inappropriately influence or bias the content of this paper.

## Acknowledgments

This research was supported in part by grant NSC-98-2313-B-005-012 from the

National Science Council, grant COA-97-6.2.1-U1(9) from the Council of Agriculture, and the Ministry of Education, Taiwan, Republic of China, under the ATU plan.

## References

Benacerraf, B.R., Benson, C.B., Abuhamad, A.Z., Copel, J.A., Abramowicz, J.S., Devore, G.R., Doubilet, P.M., Lee, W., Lev-Toaff, A.S., Merz, E., Nelson, T.R., O'Neill, M.J., Parsons, A.K., Platt, L.D., Pretorius, D.H., Timor-Tritsch, I.E., 2005. Three- and 4-dimensional ultrasound in obstetrics and gynecology: proceedings of the American Institute of Ultrasound in Medicine Consensus Conference. Journal of Ultrasound in Medicine 24, 1587-1597.

Chuang, Y.H., Chuang, W.L., Chen, S.S., Huang, C.H., 2000. Expression of transforming growth factor-beta1 and its receptors related to the ureteric fibrosis in a rat model of obstructive uropathy. The Journal of Urology 163, 1298-1303.

Corman, B., Pratz, J., Poujeol, P., 1985. Changes in anatomy, glomerular filtration, and solute excretion in aging rat kidney. The American Journal of Physiology 248, R282-287.

de Lima, V.M., Oliveira, C.P., Alves, V.A., Chammas, M.C., Oliveira, E.P., Stefano, J.T., de Mello, E.S., Cerri, G.G., Carrilho, F.J., Caldwell, S.H., 2008. A rodent model of NASH with cirrhosis, oval cell proliferation and hepatocellular carcinoma. Journal of Hepatology 49, 1055-1061.

Di Stefano, G., Fiume, L., Baglioni, M., Bolondi, L., Chieco, P., Kratz, F., Pariali, M., Rubini, G., 2008. Efficacy of doxorubicin coupled to lactosaminated albumin on rat hepatocellular carcinomas evaluated by ultrasound imaging. Digestive and Liver Disease 40, 278-284.

Dias, J.V., Paredes, B.D., Mesquita, L.F., Carvalho, A.B., Kozlowski, E.O., Lessa, A.S., Takiya, C.M., Resende, C.M., Coelho, H.S., Campos-de-Carvalho, A.C., Rezende, G.F., Goldenberg, R.C., 2008. An ultrasound and histomorphological analysis of experimental liver cirrhosis in rats. Brazilian Journal of Medical and Biological Research 41, 992-999.

Feldman, S., Brunner, L.J., 1994. Small animal model of weightlessness for pharmacokinetic evaluation. Journal of Clinical Pharmacology 34, 677-683.

Fleck, M., Appenroth, D., Malich, A., Stein, G., Fleck, C., 2002. Renal interstitial fibrosis (RIF): II. Ultrasound follow up study of single uranyl nitrate administration causing renal dysfunction in rats--comparison with histologic and functional renal parameters. Experimental and Toxicologic Pathology 54, 15-23.

Foster, F.S., Pavlin, C.J., Harasiewicz, K.A., Christopher, D.A., Turnbull, D.H., 2000. Advances in ultrasound biomicroscopy. Ultrasound in Medicine and Biology 26, 1-27.

Foster, F.S., Zhang, M.Y., Zhou, Y.Q., Liu, G., Mehi, J., Cherin, E., Harasiewicz, K.A., Starkoski, B.G., Zan, L., Knapik, D.A., Adamson, S.L., 2002. A new ultrasound instrument for in vivo microimaging of mice. Ultrasound in Medicine and Biology 28, 1165-1172.

Goertz, D.E., Yu, J.L., Kerbel, R.S., Burns, P.N., Foster, F.S., 2003. High-frequency 3-D color-flow imaging of the microcirculation. Ultrasound in Medicine and Biology 29, 39-51.

Grassi, R., Cavaliere, C., Cozzolino, S., Mansi, L., Cirillo, S., Tedeschi, G., Franchi, R., Russo, P., Cornacchia, S., Rotondo, A., 2009. Small animal imaging facility: new perspectives for the radiologist. La Radiologia Medica 114, 152-167.

Jaimes, E.A., Tian, R.X., Joshi, M.S., Raij, L., 2009. Nicotine augments glomerular injury in a rat model of acute nephritis. American Journal of Nephrology 29, 319-326.

Knspik, D.A., Starkoski, B., Pavlin, C.J., Foster, F.S., 2000. A 100-200 MHz ultrasound biomicroscope. IEEE Transactions on Ultrasonics, Ferroelectrics, and Frequency Control 47, 1540-1549.

Kogure, K., Ishizaki, M., Nemoto, M., Kuwano, H., Makuuchi, M., 1999. A comparative study of the anatomy of rat and human livers. Journal of Hepato-Biliary-Pancreatic Surgery 6, 171-175.

Kpodonu, J., Ramaiah, V.G., Diethrich, E.B., 2008. Intravascular ultrasound imaging as applied to the aorta: a new tool for the cardiovascular surgeon. The Annals of Thoracic Surgery 86, 1391-1398.

Lee, G.P., Jeong, W.I., Jeong, D.H., Do, S.H., Kim, T.H., Jeong, K.S., 2005. Diagnostic evaluation of carbon tetrachloride-induced rat hepatic cirrhosis model. Anticancer Research 25, 1029-1038.

Lu, S.C., Ramani, K., Ou, X., Lin, M., Yu, V., Ko, K., Park, R., Bottiglieri, T., Tsukamoto, H., Kanel, G., French, S.W., Mato, J.M., Moats, R., Grant, E., 2009. S-adenosylmethionine in the chemoprevention and treatment of hepatocellular carcinoma in a rat model. Hepatology 50, 462-471.

Madrahimov, N., Dirsch, O., Broelsch, C., Dahmen, U., 2006. Marginal hepatectomy in the rat: from anatomy to surgery. Annals of Surgery 244, 89-98.

Mamou, J., Aristizabal, O., Silverman, R.H., Ketterling, J.A., Turnbull, D.H., 2009. High-frequency chirp ultrasound imaging with an annular array for ophthalmologic and small-animal imaging. Ultrasound in Medicine and Biology 35, 1198-1208.

Martins, P.N., Neuhaus, P., 2007. Surgical anatomy of the liver, hepatic vasculature and bile ducts in the rat. Liver International 27, 384-392.

Morehouse, H.T., Levee, E., States, L., Zimmerman, J., Newhouse, J.H., Amis, E.S., Jr., 1995. MRI anatomy of the rat kidney at 1.5 T in different states of hydration. Magnetic Resonance Imaging 13, 81-88.

Mostbeck, G.H., Zontsich, T., Turetschek, K., 2001. Ultrasound of the kidney: obstruction and medical diseases. European Radiology 11, 1878-1889.

Nylund, K., Odegaard, S., Hausken, T., Folvik, G., Lied, G.A., Viola, I., Hauser, H., Gilja, O.H., 2009. Sonography of the small intestine. World Journal of Gastroenterology 15, 1319-1330.

Oh, J.Y., Jeong, J.S., Kim, Y.J., Nam, K.J., Park, B.H., Kwon, E.Y., Kim, Y.H., Hwang, T.H., 2002. Ultrasonographic evidence of phenotypic instability during hepatocarcinogenesis in N-nitrosomorpholine-treated rats. Experimental and

Molecular Pathology 73, 67-73.

Poltorak, A., He, X., Smirnova, I., Liu, M.Y., Van Huffel, C., Du, X., Birdwell, D., Alejos, E., Silva, M., Galanos, C., Freudenberg, M., Ricciardi-Castagnoli, P., Layton, B., Beutler, B., 1998. Defective LPS signaling in C3H/HeJ and C57BL/10ScCr mice: mutations in Tlr4 gene. Science 282, 2085-2088.

Robinson, P., 2008. Hepatocellular carcinoma: development and early detection. Cancer Imaging 8 Suppl A, S128-131.

Sullivan, J.C., Wang, B., Boesen, E.I., D'Angelo, G., Pollock, J.S., Pollock, D.M., 2009. Novel use of ultrasound to examine regional blood flow in the mouse kidney. American Journal of Physiology. Renal Physiology 297, F228-235.

Taylor, K.J., Carpenter, D.A., Hill, C.R., McCready, V.R., 1976. Gray scale ultrasound imaging. The anatomy and pathology of the liver. Radiology 119, 415-423.

Tsai, T.H., Yang, P.C., 2003. Ultrasound in the diagnosis and management of pleural disease. Current Opinion in Pulmonary Medicine 9, 282-290.

Van Rhijn, I., Godfroid, J., Michel, A., Rutten, V., 2008. Bovine tuberculosis as a model for human tuberculosis: advantages over small animal models. Microbes and Infection 10, 711-715.

Wieckowska, A., Feldstein, A.E., 2008. Diagnosis of nonalcoholic fatty liver disease: invasive versus noninvasive. Seminars in Liver Disease 28, 386-395.

Yan, G., Duan, Y., Ruan, L., Yang, Y., Cao, T., 2007. Experimental study on the relation between the noninvasive ultrasonography quantitative scoring system and the degree of the hepatic fibrosis. Hepato-Gastroenterology 54, 1908-1914.

Yang, P.C., 2000. Ultrasound-guided transthoracic biopsy of the chest. Radiologic Clinics of North America 38, 323-343.

Yang, R., Kopecky, K.K., Rescorla, F.J., Galliani, C.A., Grosfeld, J.L., 1993. Changes of hepatoma echo patterns with tumor growth. A study of the microanatomic basis in a rat model. Investigative Radiology 28, 507-512.

435 Yen, C.C., Lin, C.Y., Chong, K.Y., Tsai, T.C., Shen, C.J., Lin, M.F., Su, C.Y., Chen,
436 H.L., Chen, C.M., 2009. Lactoferrin as a natural regimen for selective
437 decontamination of the digestive tract: recombinant porcine lactoferrin
438 expressed in the milk of transgenic mice protects neonates from pathogenic
439 challenge in the gastrointestinal tract. The Journal of Infectious Diseases 199,
440 590-598.
441

**Table 1.**

**Sonographic comparison of rat and human abdominal organs**

| Rat | Human |
|---|---|
| Kidneys | |
| Right kidney is superior to left kidney | Left kidney is superior to right kidney |
| Easy to scan in supine position | Relatively difficult to obtain ideal view, sometimes need decubitus position from the flanks |
| Lack of obvious border between the medulla and the cortex | Strongly echogenic (medulla) in central portion with hypoechoic surroundings (cortex) |
| Easy to view supplying blood vessels passing through the kidneys | Hard to view supplying blood vessels passing through the kidneys |
| Liver | |
| Gallbladder absent | Gallbladder present |
| Multilobed liver with clear fissures | Liver lobes have no clear fissure lines or divisions |
| Right liver border is shaped like a C-curve | Right liver border is wedge-shaped |
| Easy to deform by compression | Shape unchanged by compression |

**Figure legends**

Fig. 1. Anatomy of rat abdominal organs after removal of stomach and intestines. RML, right medial lobe; LML, left medial lobe; LLL, left lateral lobe; SRL, superior right lobe; IRL, inferior right lobe; RK, right kidney; LK, left kidney; IVC, inferior vena cava.

Fig. 2. Ultrasonographic demonstration of the right kidney in longitudinal section by different angles of 40-MHz transducer sweeps through a sonic window. (a) Cartoon diagram of stereo location of right kidney detected by different scanning angles (shown as arrow b and arrow c) of transducer sweeps. (b) Right kidney (RK) sits just below the inferior right lobe (IRL) of the liver. (c) The parenchyma comprises the relatively hypoechoic medullary pyramids, which lie centrally. (d) A schematic diagram of (b). IRL, inferior right lobe; RK, right kidney. (e) A schematic diagram of (c). SL, skin layer; ML, muscle layer; RRA, right renal artery; RRV, right renal vein; RC, renal capsule.

Fig. 3. Ultrasonographic demonstration (40-MHz) of the vessels below the liver in transverse section. (a) Cartoon diagram of space distribution of celiac artery round as shown with an arrow. (b) The ultrasound of hepatic portal area and celiac artery round.

(c) A schematic diagram of (b). CBD, common bile duct; HA, hepatic artery; PV, portal vein; IRL, inferior right lobe of the liver; IVC, inferior vena cava.

Fig. 4. Ultrasonographic demonstration (40-MHz) of the right part of the liver in transverse section. (a) Cartoon diagram of space distribution of liver and celiac artery round. Images (b) and (c) were produced using different angles of transducer sweeps through a sonic window. Image (d) was a slightly left-shifted scan. (e) A schematic diagram of (b). RML, right medial lobe; M, margin of the right liver. (f) A schematic diagram of (c). HV, hepatic vein; PV, portal vein. (g) A schematic diagram of (d). RML, right medial lobe; F, fissure; SRL, superior right lobe.

Fig. 5. Ultrasonographic demonstration (40-MHz) of the middle part of the liver in transverse section. (a) Cartoon diagram of space distribution of the middle liver. (b) Superficial view. (c) Deep view of the same transverse section after transducer compression. (d) A schematic diagram of (b). LML, left medial lobe; RML, right medial lobe; F, fissure between LML and RML. (e) A schematic diagram of (c). LLL, left lateral lobe; PT, portal triad; A, aorta.

Fig. 6. Ultrasonographic demonstration of the left part of the liver in transverse

section using different angles of 40-MHz transducer sweeps through a sonic window. (a) Cartoon diagram of space distribution of the left liver and stomach. (b) Superior view. (c) Inferior view. (d) A schematic diagram of (b). LLL, left lateral lobe; M, margin of the LLL. (e) A schematic diagram of (c). LLL, left lateral lobe; S, stomach.

Fig. 7. Ultrasonographic demonstration (40-MHz) of the spleen in longitudinal section. (a) Cartoon diagram of space distribution of spleen and celiac round. (b) Inferior part of the left spleen. (c) A schematic diagram of (b). Sp, spleen.

Fig. 8. Ultrasonographic demonstration (5-MHz) of human liver, gallbladder, spleen, and right kidney. L: liver; GB: gallbladder; K: kidney; Sp: spleen.

**Figure 1**

Click here to download high resolution image

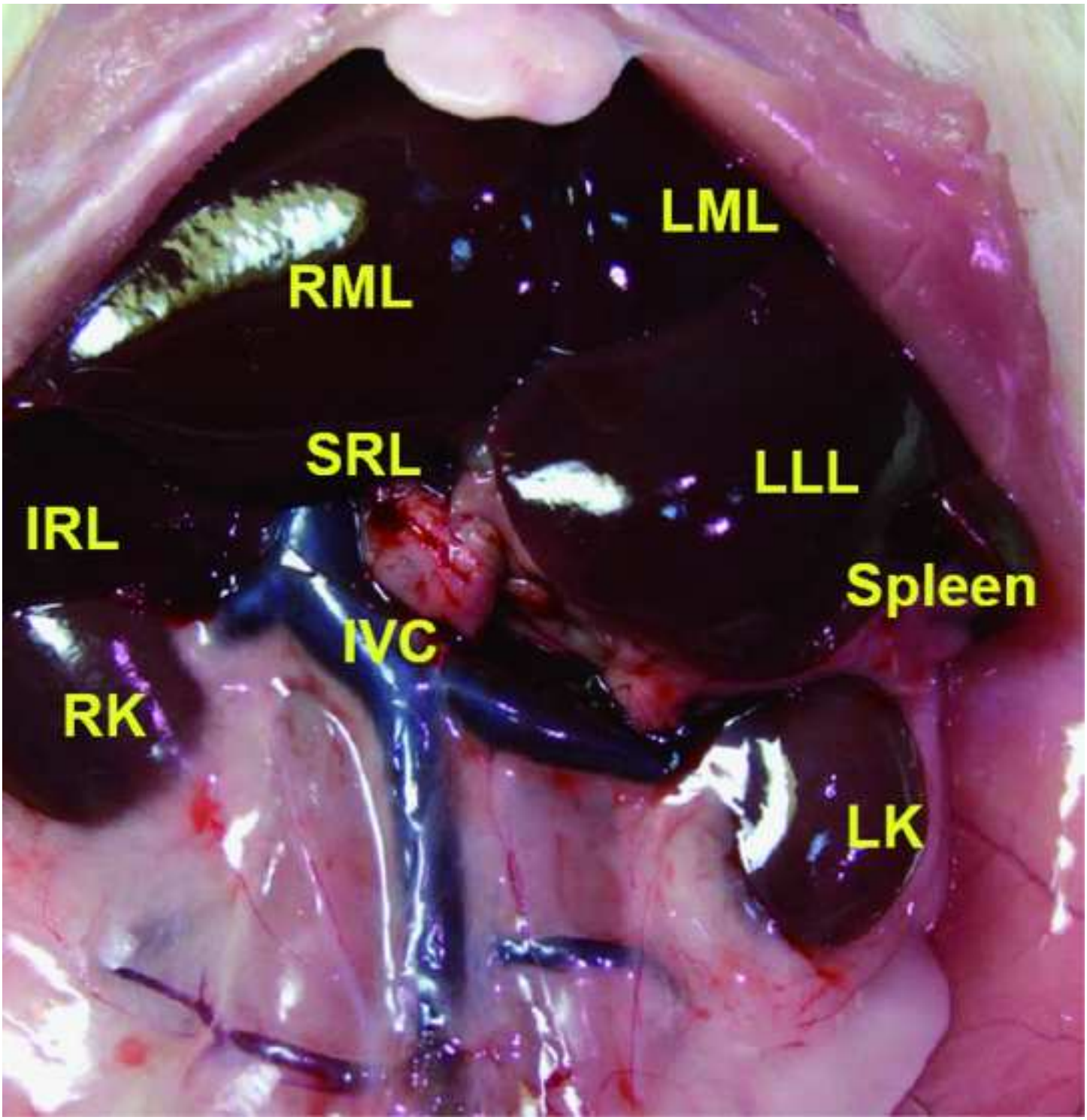

Figure 2

Click here to download high resolution image

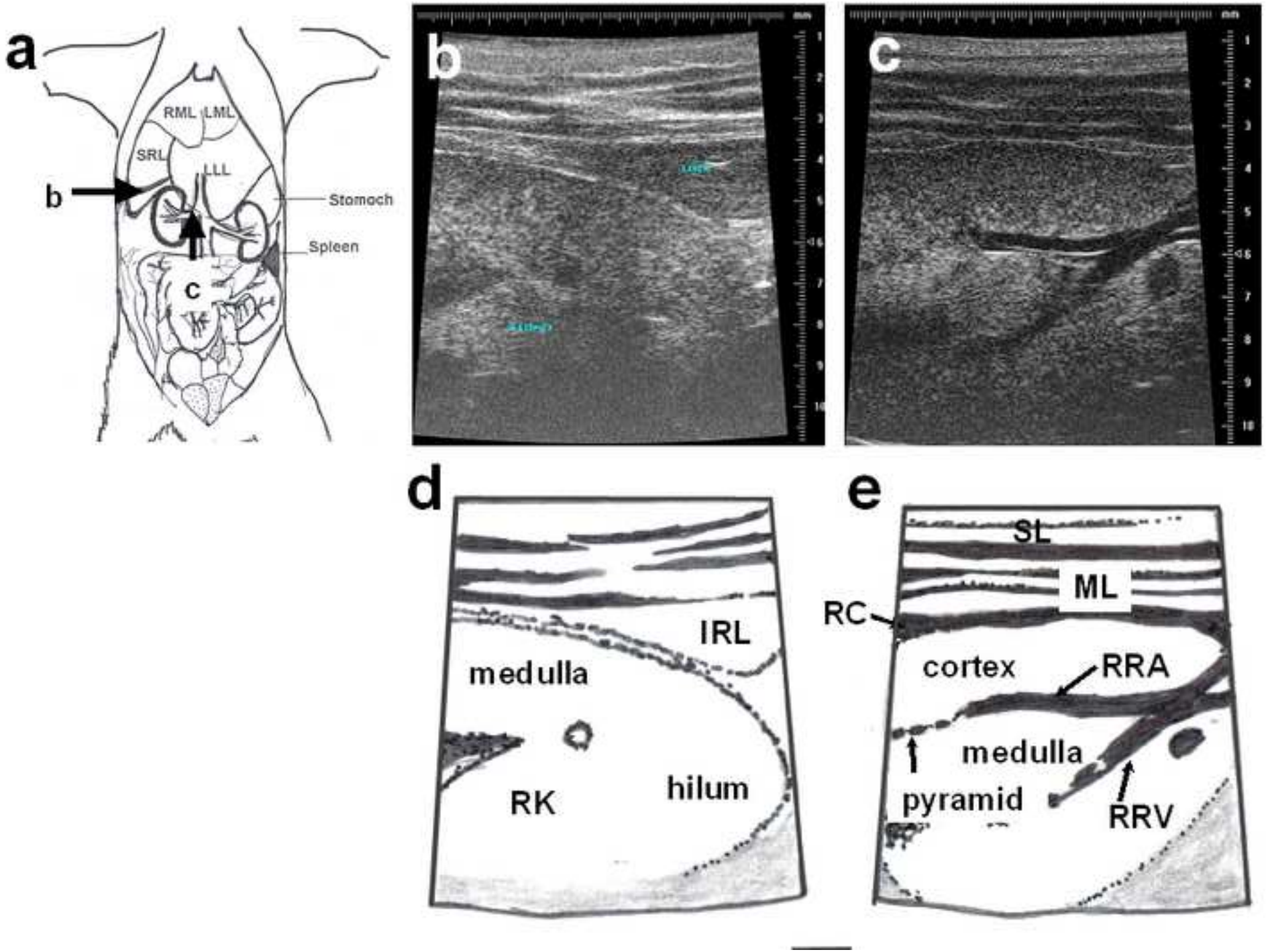

**Figure 3**

Click here to download high resolution image

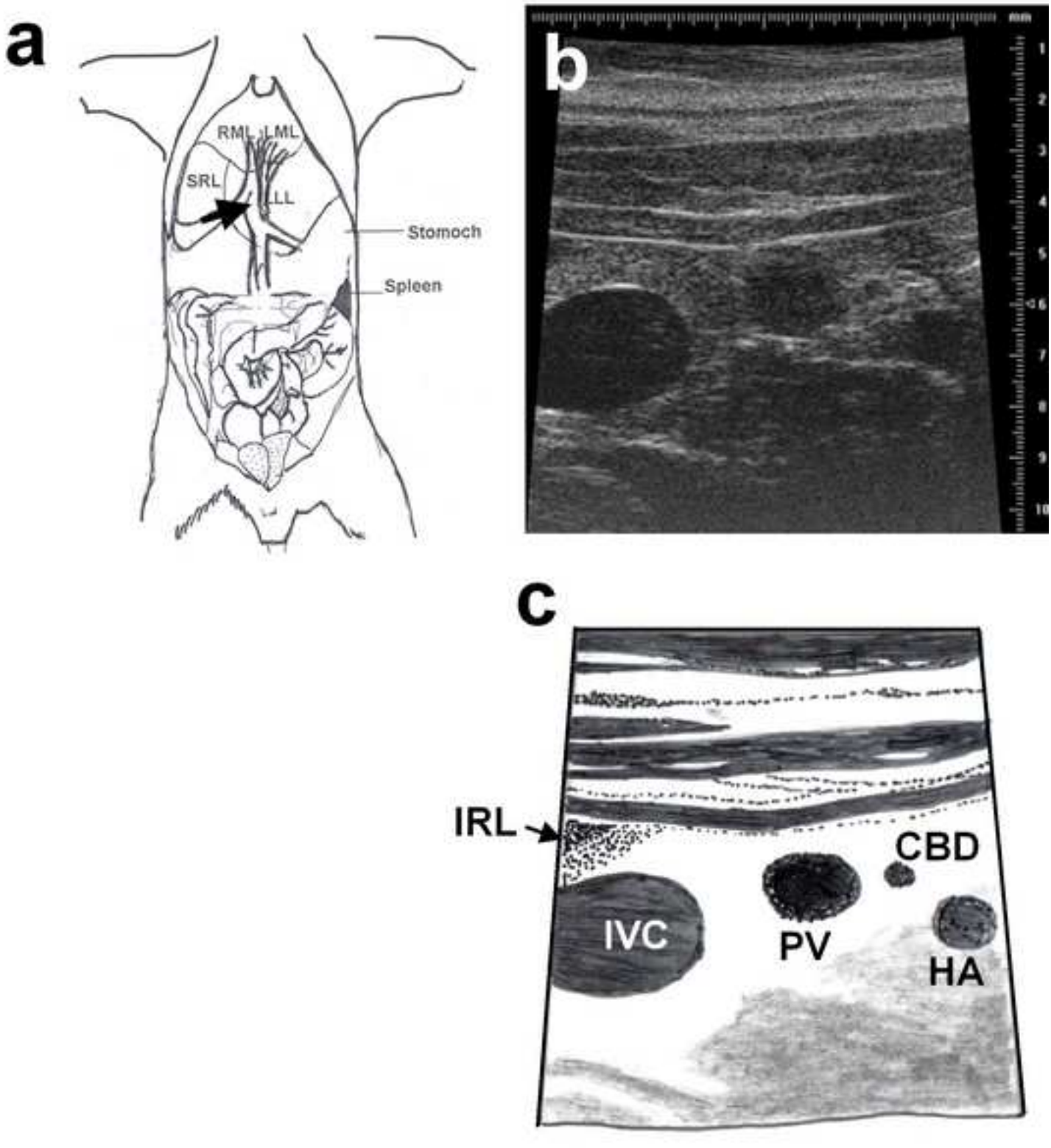

**Figure 4**

Click here to download high resolution image

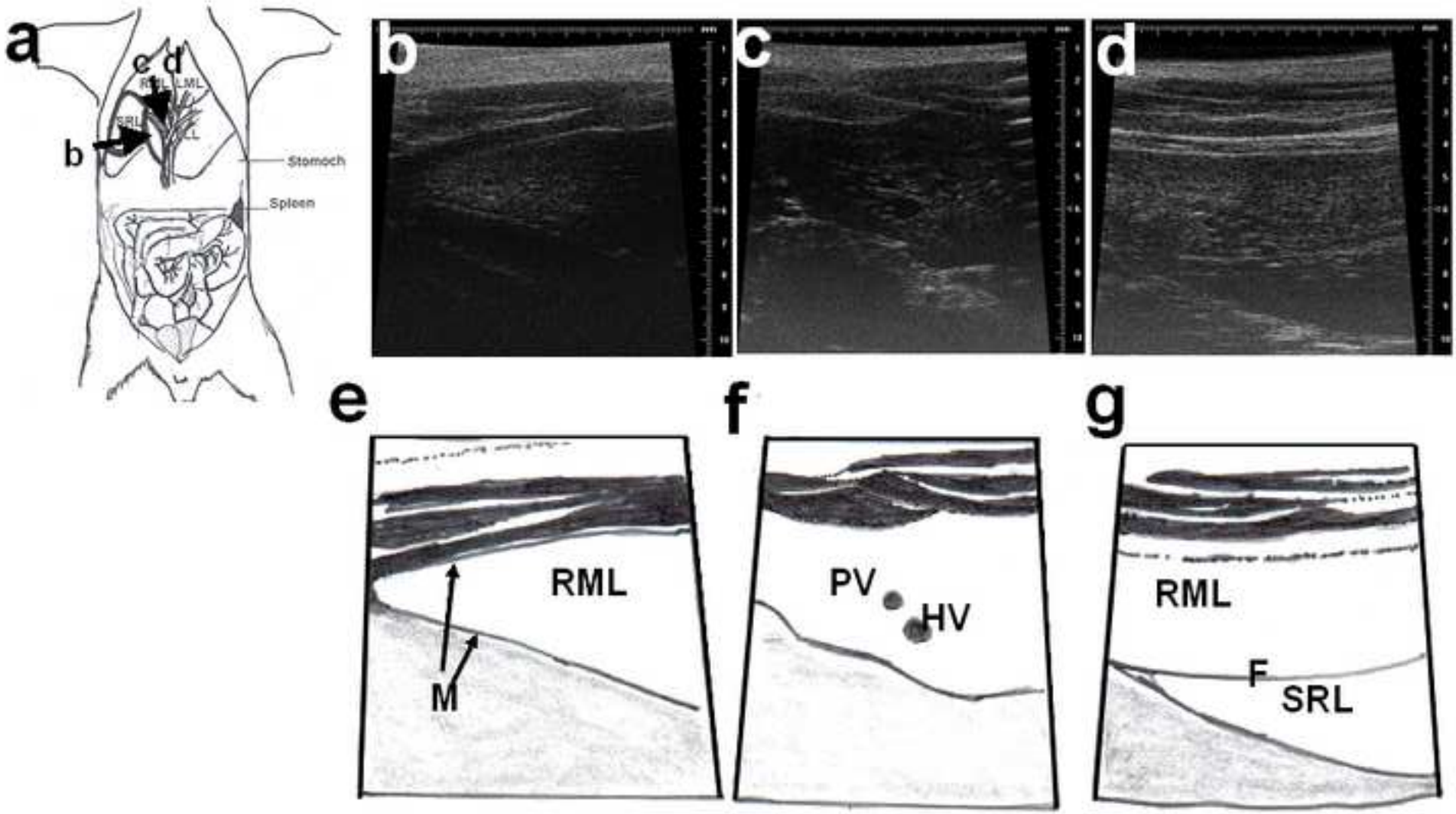

**Figure 5**

Click here to download high resolution image

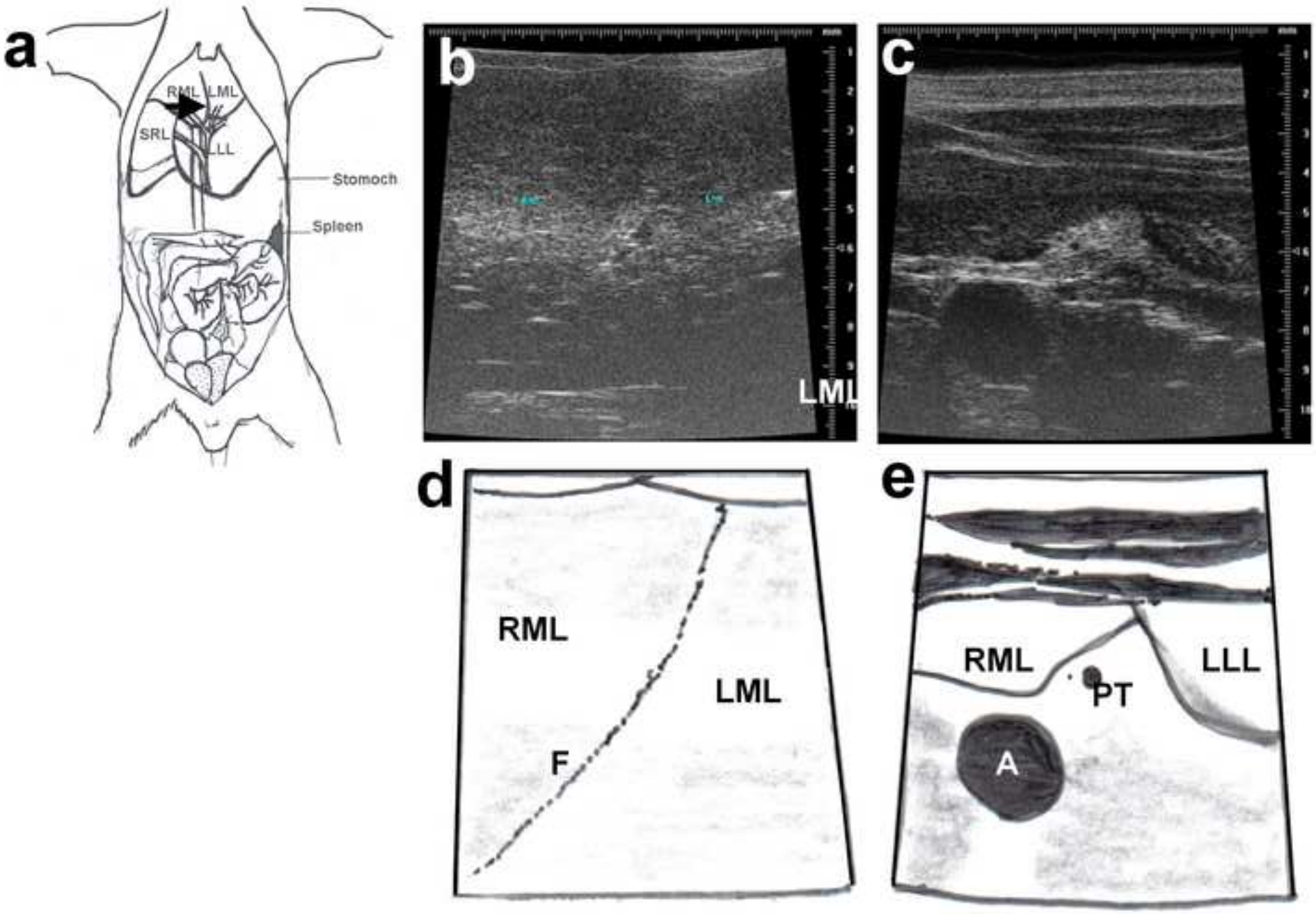

Figure 6

Click here to download high resolution image

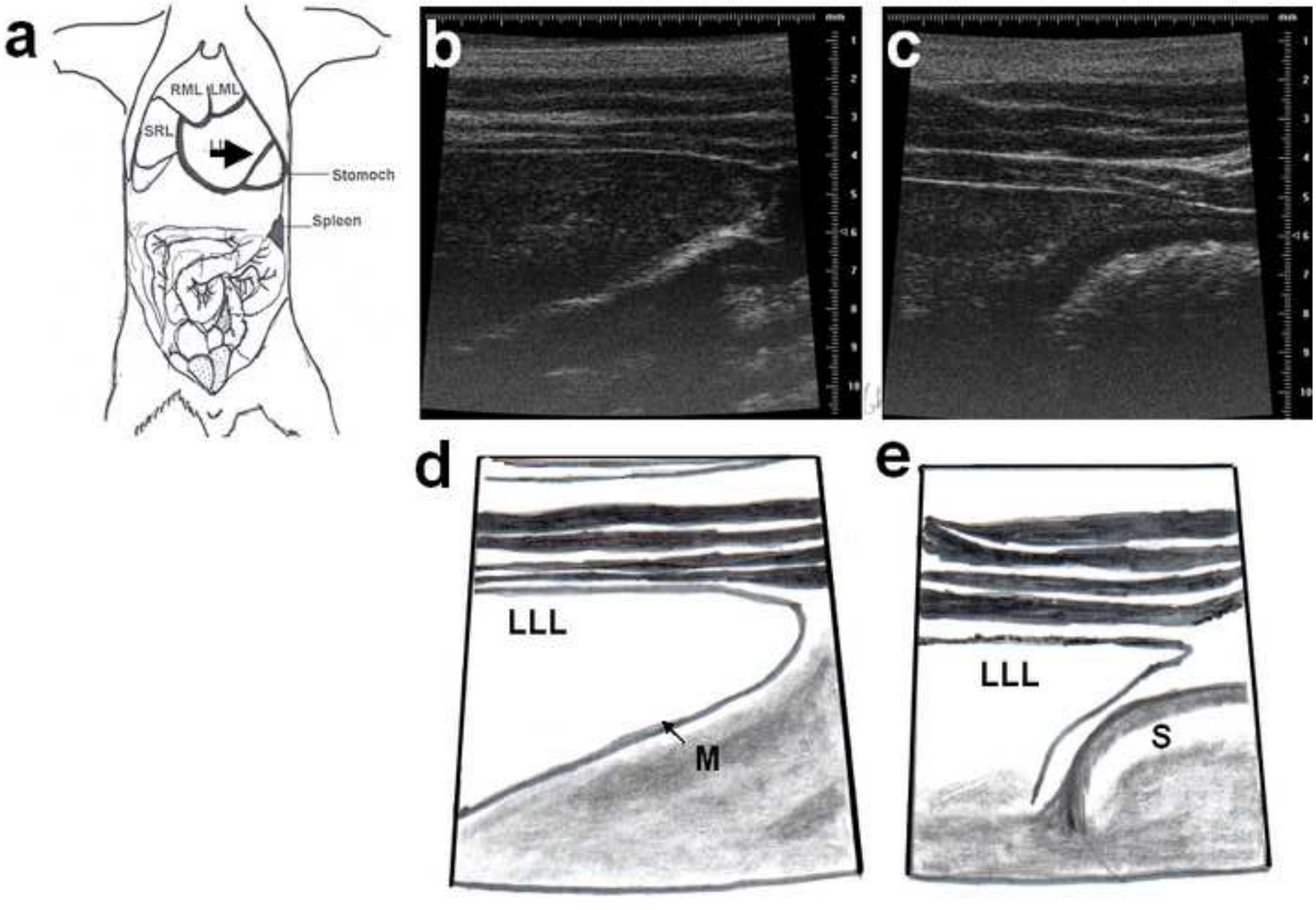

**Figure 7**

Click here to download high resolution image

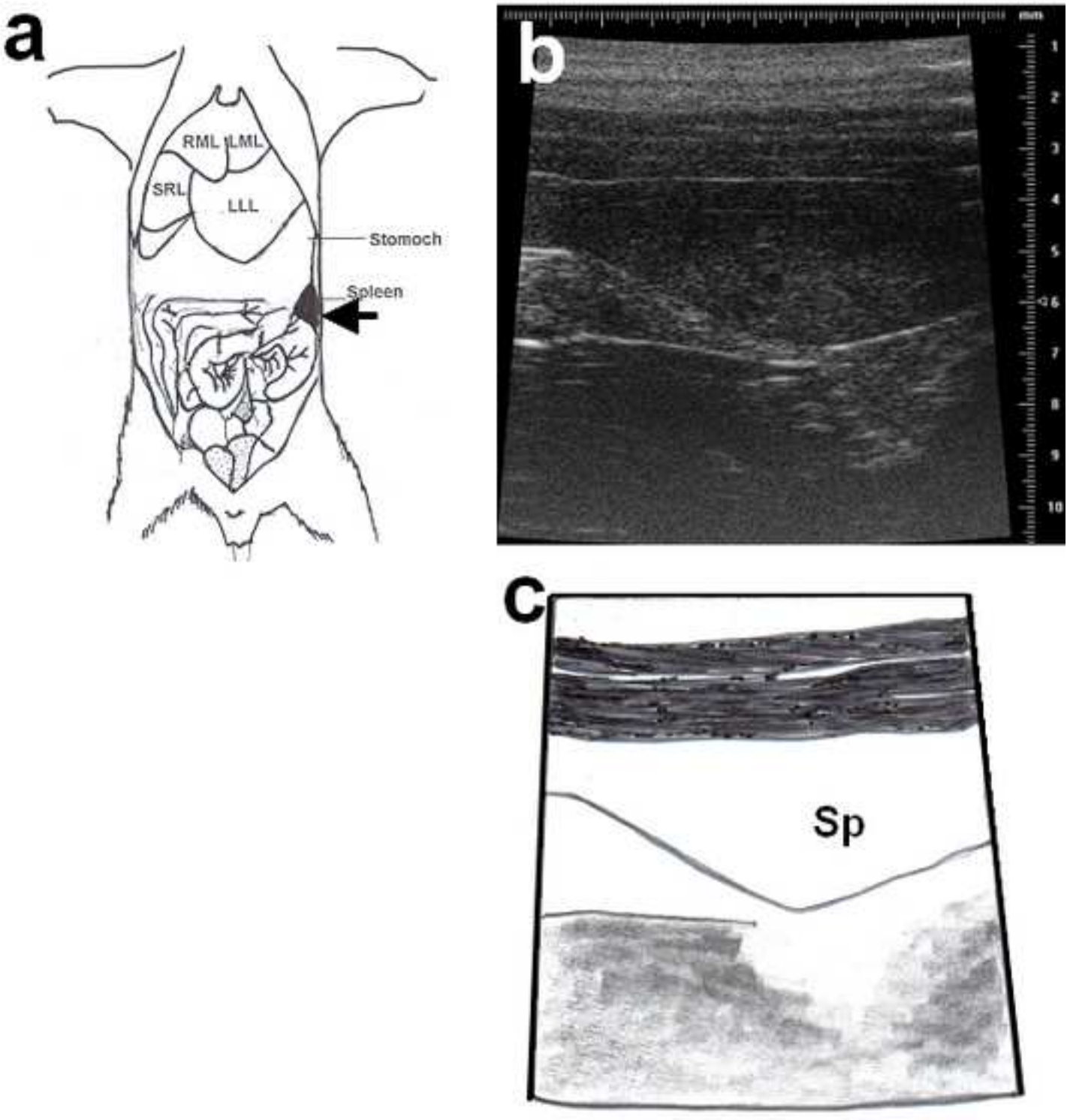

**Figure 8**

Click here to download high resolution image

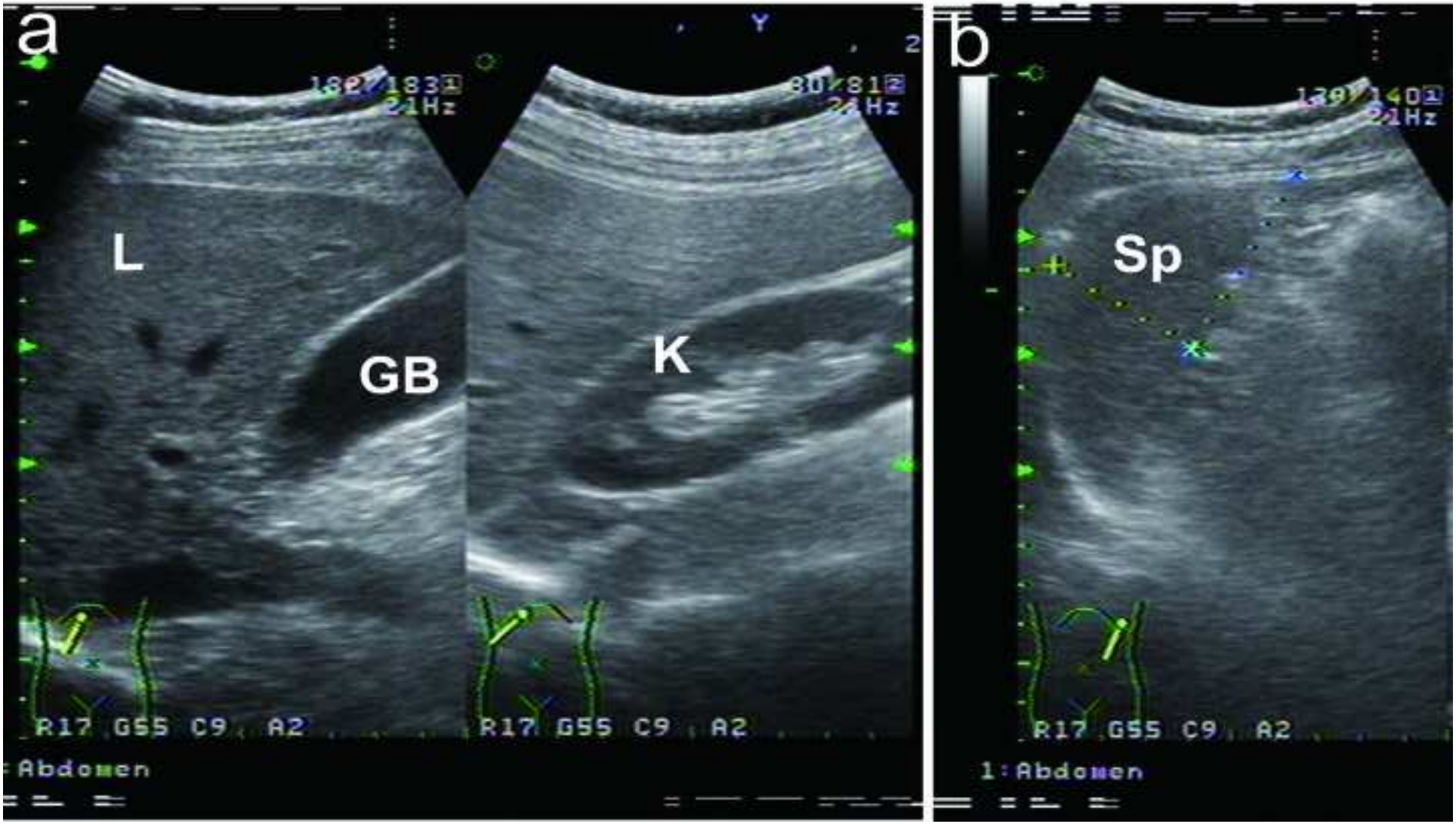

國立中興大學 National Chung Hsing University http://www.nchu.edu.tw 250, Kuo-Kuang Road, Taichung 402, Taiwan

# Modifications and revisions

**Thank you very much for Reviewers' valuable opinions. The paper was revised based upon your constructive suggestions. And the followings are the point-by-point response to your comments:**

## For reviewer #1:

**Q1.** What RMV scan head was used for the ultrasound analysis?
**Answer:** The mode of RMV scan head is "RMV-704". The information has been added in the description in the Materials and methods section (Lines 107-108) as followed: "Therefore, a commercially available HFU apparatus (Visual Sonics Vevo 770 with the RMV 704) was used in this experiment".

**Q2.** Were the animals fasted prior to scanning to limit intestinal motions during the imaging?
**Answer:** Yes, the animals were fasted for 3 h prior to high-frequency ultrasound (HFU) scanning. This description has been added in the HFU examination paragraph of Materials and Methods section (Lines 101-102).
.

**Q3.** Why not use the aorta as a structural landmark?
**Answer:** In gray scale, it is not easy to differentiate the aorta from other vascular system, such as inferior vena cava, portal vein or hepatic artery because all of them appear as simple hypoechoic tubular structures under transverse view. In our experience, the right kidney is a good landmark for the initiation of ultrasonic scanning because of its particular structure (oval-shape with relatively hyperechogenic central portion) and easy approach.

**Q4.** Is the imaging done free hand or using the rail system?
**Answer:** The HFU imaging was done by free hand operation as the same situation of clinical ultrasound scanning. In this study, Two HFU operators were applied, one is a well-trained HFU expertise (Mr. Jiun-Yu Chen) and the other is a clinical medical doctor (Dr. Wei Chen). All of the HFU images were double check between these two operators.

**Q5.** Is the gating feature used?
**Answer:** No gating feature was used in this study.

**Q6.** For ALL images I would suggest including a panels for each figure with I of the panels showing a clear outline of the structure of interest. Even for people accustomed to looking at ultrasound images it is difficult to "find" what the authors are trying to highlight.
**Answer:** According to reviewer's suggestion, all the HFU images of figures 2-7 were added the panels showing a clear outline of the structures of interest. The abbreviation labels in the interpretive diagrams were also described in the figure legends.

**Q7.** Line 161, I believe there is a problem with the weight of the rats as stated. The liver's weigh 12.5 g but the rats weigh 9.6-13.5 g.
**Answer:** The meaning is a range of liver weights between 9.6 and 13.5 g, but our description was unclear. The sentence has been revised as followed: "In rat liver weighting range from 9.6 to 13.5 g, the liver's mean weight was 12.5 g".

## For reviewer #2:

**Q1.** Abstract - Change "in vitro scanning" to "in situ scanning".
**Answer:** According to reviewer's suggestion, the term of "in vitro scanning" has been changed to "in situ scanning" (Line 27 in the Abstract section).

**Q2.** Typographical error on line 87: "12-sh"
**Answer:** The typographical error of "12-sh" has been corrected as "12-h".

**Q3.** Line 136 - change measurement units to mm to be consistent with the diameters given below.
**Answer:** The measurement units have been changed as "….between 8 and 10 mm".

**Q4.** Line 161 - the sentence regarding rat weights doesn't quite make sense. Please check this.
**Answer:** The meaning is a range of liver weights between 9.6 and 13.5 g, but our description was unclear. The sentence has been revised as followed: "In rat liver weighting range from 9.6 to 13.5 g, the liver's mean weight was 12.5 g".

**Q5.** Line 271 - consider changing the word "development" to "employment" or similar.
**Answer:** The word of "development" has been changed to "employment".

**Q6.** Line 274-5 - this study did not examine liver regeneration or the ability of ultrasound to

detect progress in liver regeneration. The authors should re-word this sentence accordingly.

**Answer:** The sentence has been revised as followed: "By the knowledge, we may observe the process of tissue regeneration or severity of tissue injury of the abdominal organs more accurately in the future."

**Q7.** Figure labeling: Would it be possible to avoid using the same numbers for different anatomical features within the same figure? For example, in Figure 5, the number 2 indicates the right medial lobe in Fig. 5a but the portal triad in Fig 5b. This is a little confusing. Using the abbreviations (e.g. LML) rather than numbers on the figures might be easier to understand at a glance.

**Answer:** To avoid the confusing of the numbers labeling, all of the labels have been revised using the abbreviations as shown in Figures 1 to 8 and their figure legends.

**Q8.** Table 1: Consider changing "Unobvious" to "Lack of obvious"

**Answer:** According to reviewer's suggestion, the word of "Unobvious" has been revised as "Lack of obvious ".

國立中興大學
National Chung Hsing University
http://www.nchu.edu.tw
250, Kuo-Kuang Road, Taichung 402, Taiwan

**Dr. Andrew Higgins** **Nov. 17, 2010**
**Editor-in-Chief**
**The Veterinary Journal**

**Dear Editor Higgins:**

**Thank you and the referees for your careful consideration of our manuscript entitled *"Application of high-frequency ultrasound for the detection of surgical anatomy in the rodent abdomen"* coded YTVJL-D-10-00623R1. Following your helpful comments, we have enumerated our responses to the reviewers' comments and modified our manuscript accordingly.**

**Please find two attached files including a list of the modifications to the original manuscript and our replies to the comments, and a full-text of the revised manuscript. We are confident that this revised paper is now suitable for publication in the *Veterinary Journal*.**

**We are looking forward to hearing from you and deeply appreciate your kindly help!**

**Yours sincerely,**

**Chuan-Mu Chen, Ph.D.**
**Professor / Dean**
**Department of Life Sciences**
**National Chung Hsing University**
**250 Kuo Kuang Road, Taichung**
**402, Taiwan**
**TEL: 886-4-2285-6309**
**FAX: 886-4-2287-4740**
**E-mail: chchen1@dragon.nchu.edu.tw**